Virology 402 (2010) 355–365

Contents lists available at ScienceDirect

Virology

journal homepage: www.elsevier.com/locate/yviro

The tripartite capsid gene of *Salmonella* phage Gifsy-2 yields a capsid assembly pathway engaging features from HK97 and λ

Grégory Effantin [a,1], Nara Figueroa-Bossi [b], Guy Schoehn [a,c], Lionello Bossi [b], James F. Conway [a,d,*]

[a] Laboratoire de Microscopie Electronique Structurale, Institut de Biologie Structurale J.-P. Ebel, UMR 5075, Université Joseph Fourier, CEA, CNRS, 38027 Grenoble, France
[b] Centre de Génétique Moléculaire, CNRS, 91198 Gif-sur-Yvette, France
[c] Unit for Virus Host Cell Interaction, UMI 3265, Université Joseph Fourier, EMBL, CNRS, 38042 Grenoble, France
[d] Department of Structural Biology, University of Pittsburgh School of Medicine, Pittsburgh, PA 15260, USA

ARTICLE INFO

Article history:
Received 13 January 2010
Returned to author for revision
8 February 2010
Accepted 23 March 2010
Available online 28 April 2010

Keywords:
Bacteriophage
Gifsy-2
Capsid
Cryoelectron microscopy
Phage
Lambda
HK97
Structure
Assembly
Electron microscopy

ABSTRACT

Phage Gifsy-2, a lambdoid phage infecting *Salmonella*, has an unusually large composite gene coding for its major capsid protein (mcp) at the C-terminal end, a ClpP-like protease at the N-terminus, and a ~200 residue central domain of unknown function but which may have a scaffolding role. This combination of functions on a single coding region is more extensive than those observed in other phages such as HK97 (scaffold–capsid fusion) and λ (protease–scaffold fusion). To study the structural phenotype of the unique Gifsy-2 capsid gene, we have purified Gifsy-2 particles and visualized capsids and procapsids by cryoelectron microscopy, determining structures to resolutions up to 12 Å. The capsids have lambdoid T = 7 geometry and are well modeled with the atomic structures of HK97 mcp and phage λ gpD decoration protein. Thus, the unique Gifsy-2 capsid protein gene yields a capsid maturation pathway engaging features from both phages HK97 and λ.

Introduction

Tailed icosahedral phages dominate the biosphere (Hendrix, 2002) and come in many morphological and structural variations. At the level of molecular morphology, phages are observed to assemble following common general principles (Fig. 1). The capsid assembly pathways of several lambdoid phages have been studied extensively, including the *Escherichia coli* bacteriophages λ (Dokland and Murialdo, 1993), HK97 (Lata et al., 2000; Ross et al., 2006), and T7 (Agirrezabala et al., 2005; Cerritelli et al., 2003) and the *Salmonella* phage P22 (Lander et al., 2006; Zhang et al., 2000). In each case, a precursor capsid (procapsid or prohead) assembles with the aid of a scaffold protein or domain into a round particle obeying icosahedral symmetry save for one vertex that is occupied by a dodecameric structure called the portal or connector. For many phages, the major capsid protein(s) are subsequently truncated at the N-terminus by a phage-encoded protease, yielding a metastable particle primed for DNA packaging and capsid expansion. The dsDNA genome is packaged through the portal, triggering expansion of the capsid into the larger and polyhedral mature form, and subsequently the tail, assembled on an independent pathway, binds to the connector. Another common but not universal step is stabilization of the expanded capsid by binding of one or more accessory proteins to the exterior surface or by covalent cross-linking between capsid protein subunits (Duda, 1998).

Further common principles are evident in capsid protein structures, such as the portals and connectors (Cardarelli et al., 2010), proteases (Cheng et al., 2004) and major capsid proteins (Bamford et al., 2005), as well as in the placement of the genes encoding these proteins in the phage genome. The head genes of smaller tailed phages are often observed in the order: portal, protease, scaffold, and major capsid protein (Hendrix and Duda, 1998). An interesting variation on this genetic architecture is the combination of two of these functions into one coding unit, such as the protease–gpC/scaffold–gpNu3 of λ (Shaw and Murialdo, 1980) and the scaffold/major capsid protein gp5 of HK97 (Duda et al., 1995). The HK97 capsid assembly pathway has been studied extensively, in part due to its tractability and simplicity.

Abbreviations: cryoEM, cryo-electron microscopy; Å, Ångstrom; bp, base pairs.

* Corresponding author. Department of Structural Biology, University of Pittsburgh School of Medicine, Biomedical Science Tower 3, Room 2047, 3501 5th Ave, Pittsburgh, PA 15260, USA. Fax: +1 412 648 8998.
E-mail address: jxc100@pitt.edu (J.F. Conway).
[1] Present address: Unit for Virus Host Cell Interaction, UMI 3265, Université Joseph Fourier, EMBL, CNRS, 38042 Grenoble, France.

0042-6822/$ – see front matter © 2010 Elsevier Inc. All rights reserved.
doi:10.1016/j.virol.2010.03.041

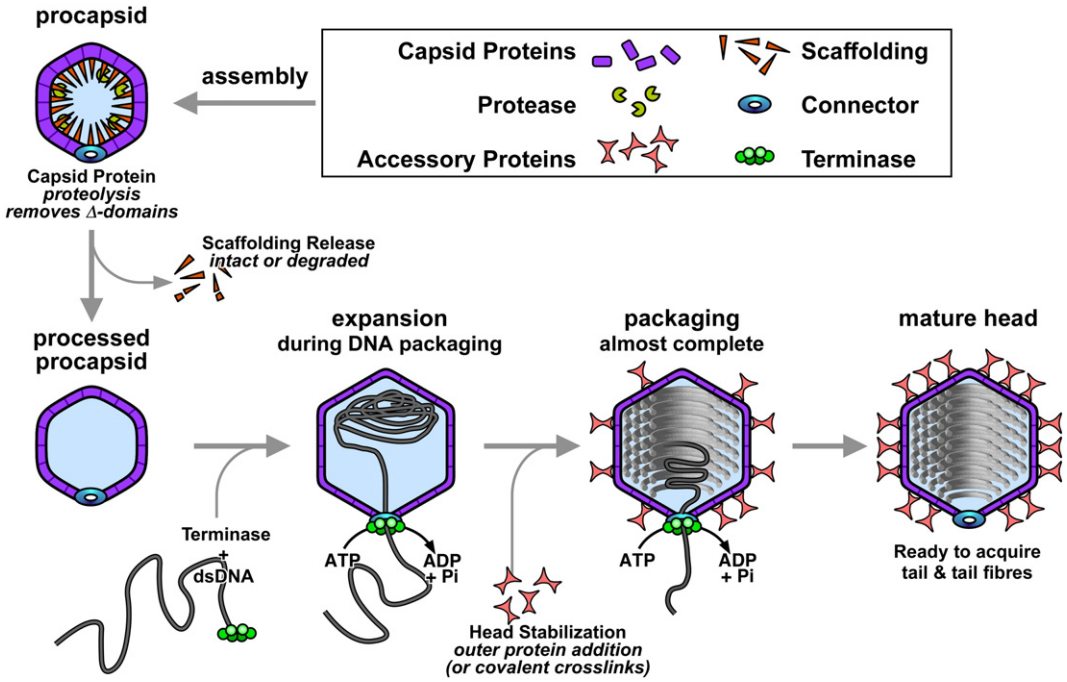

Fig. 1. Generalized capsid assembly pathway, adapted from (Steven et al., 2005). The procapsid assembles around a nucleating connector located at an icosahedral vertex, and may employ a scaffold protein, or in the case of phage HK97 a scaffold domain that is the N-terminal part of the major capsid protein. The scaffold is subsequently removed and, together with the N-terminal of the major capsid protein, may be proteolyzed. DNA packaging triggers expansion that significantly transforms the capsid and allows any stabilization mechanisms to proceed, such as binding of any accessory molecules or cross-linking between capsid protein subunits.

Expression of the capsid protein alone is sufficient for assembly of icosahedral procapsid-like particles, and co-expression with the viral protease (gp4) yields proteolyzed procapsids that may be matured to a head-like form although lacking the portal and DNA. Since the 102-residue N-terminal domain of gp5 is required for assembly, but subsequently dispensed with, its function appears to be as a guide for assembly. Genetically it is adjacent and upstream of the mcp coding region, consistent with a portal–protease–scaffold–mcp genetic order of phage structural elements but with the latter two functions fused onto one gene. This fused scaffold–mcp function is also observed in other phages, including phage T5 (Effantin et al., 2006). Phage λ presents a different combination of functions on the C/Nu3 gene—gpNu3 is the scaffold protein and is identical to the C-terminal third of the gpC protease (Hendrix and Casjens, 2006).

Here, we present our structural analysis of the lambdoid phage, Gifsy-2, that exhibits new variations on the characteristics embodied by known lambdoid phages. Gifsy-2, first identified as a prophage in the *Salmonella* strain LT2 genome (Figueroa-Bossi et al., 1997), is an active bacteriophage that can be released from strain ATCC14028 (Figueroa-Bossi and Bossi, 1999). It carries genes that contribute to bacterial virulence, such as the sodC gene (Figueroa-Bossi et al., 2001), and its discovery in different *Salmonella enterica* strains suggests that it may play a role in horizontal gene transfer between bacteria. Gifsy-2 is also capable of infection and lysogenization of *Salmonella* serovars other than *typhimurium* (Figueroa-Bossi et al., 2001). The Gifsy-2 dsDNA genome is 45.5 kb in length and shares significant similarities with other known phages (Thomson et al., 2004). In the present study, we focus on the structural genes and their products that are involved in capsid assembly. Using cryoelectron microscopy data, we have determined structures for several forms of the Gifsy-2 capsid allowing comparison with related capsids, in particular those of coliphages λ and HK97. Our bioinformatic analysis shows that Gifsy 2 has a new layout for the capsid genes in which the functions of several normally separate genes are combined into a single open reading frame. These results add to the diversity of phage assembly strategies and offer directions for future experiments that will confirm and extend the degree of connectedness between viruses of different host types and with different morphologies.

Results

Identification of Gifsy-2 major capsid protein and its gene

Induction and purification of Gifsy-2 yielded primarily procapsids, as assessed by electron microscopy. N-terminal sequencing of denatured particles allowed us to identify constituent proteins of the capsid. The strongest band had M_r ~32 kDa, a common size for the proteolyzed form of major capsid proteins of lambdoid phages, and the N-terminal was coincident with a peptide from a large gene encoding 693 amino acids (M_w ~75 kDa; GenBank NP_460008). Both the starting point for this putative capsid protein and its size are consistent with it coming from the C-terminal 292–295 amino acids of the larger protein. This region shows weak local homologies with the major head subunits of the enterobacteria phage Mu (gpT: NP_050638)—28% identity over 70 residues by BLASTP—and of phage Pnm1 (NP_284557) with 36% identity over 75 residues (Morgan et al., 2002). We conclude that this protein is the mature form of the Gifsy-2 major capsid protein and is likely a proteolyzed product of a precursor in the capsid assembly pathway.

Although proteolysis of the major capsid protein is common in lambdoid and other phage assembly pathways, the full-length precursor form of the protein is not typically so large as 75 kDa. Intriguingly, the N-terminal part of the product of this large gene shares significant sequence homology with the ClpP protease family (23% identity over 193 residues to the *E. coli* ClpP sequence solved crystallographically: PDB 1TYF (Wang et al., 1997) including alignment of Gifsy-2 residues Ser96, His119, and Asp180 with the catalytic triad of ClpP (Fig. 2). The central domain of ~200 residues has no obvious homology with other phage proteins and appears to constitute a distinct domain. Since the genes of proteins involved in assembly of phage capsids are often ordered as portal, protease, scaffold, and capsid (Hendrix and Duda, 1998), the long 75-kDa sequence appears to fulfill at least two of the functions—

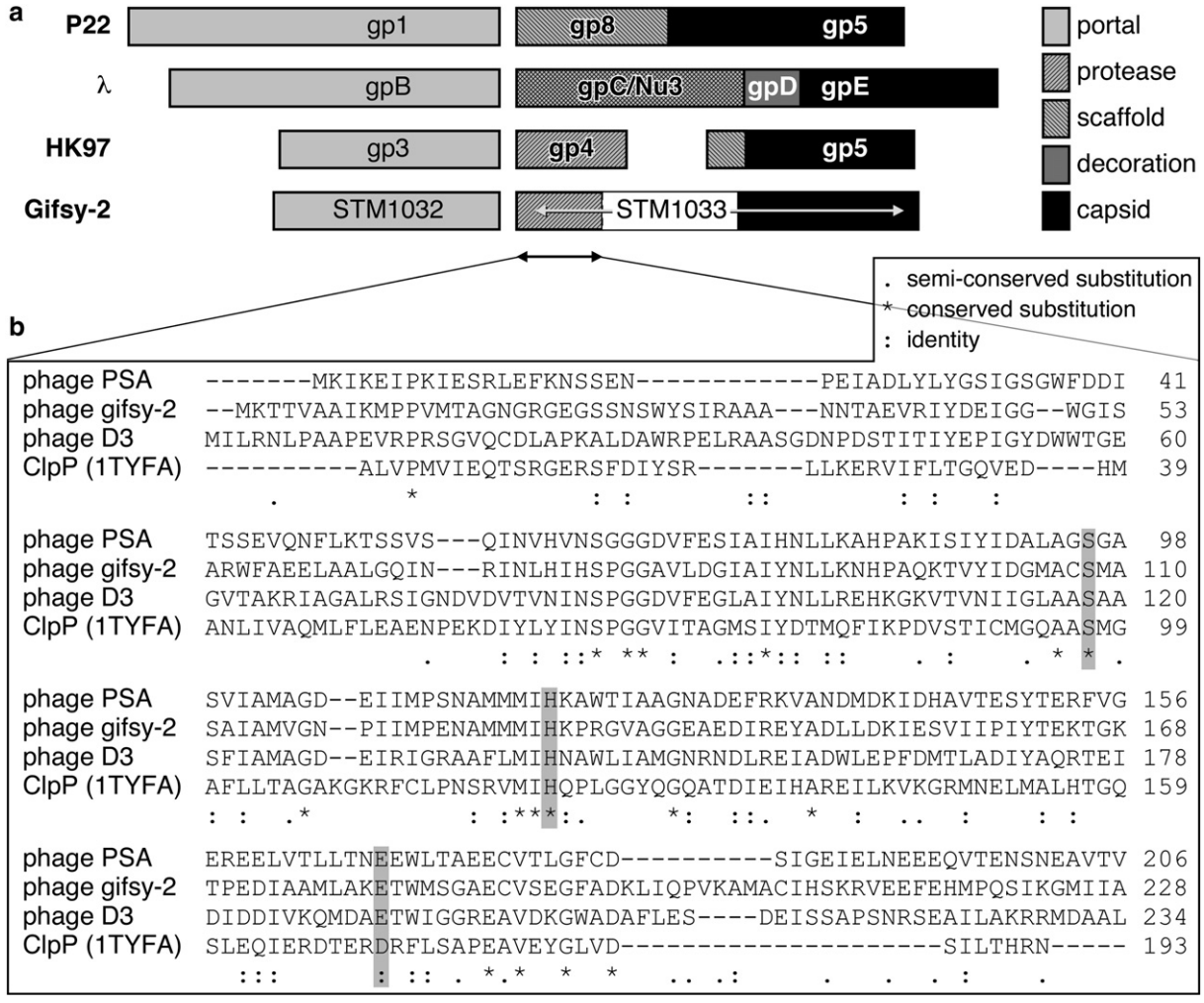

Fig. 2. (a) Structural gene organization for phages P22, λ, and HK97, and those known or inferred for Gifsy-2. Coding regions are mutually scaled—the HK97 gp3 codes for 424 amino acids. (b) ClustalW sequence alignment of the protease function of phages PSA (CAC85560), Gifsy-2 (NP_460008), D3 (AAD38956), and subunit A of the *E. coli* ClpP protease (PDB 1TYFA). Locations of the ClpP catalytic triad and residues aligned with them are shaded.

protease and capsid—and a reasonable hypothesis is that the central domain may include a scaffolding role. In keeping with the general pattern, we observe that the translated adjacent upstream gene scores most highly in BLASTP searches with phage portal proteins, including 48% identity with the λ gpB portal protein. While dual-function protease/scaffold and scaffold/capsid protein genes have already been observed (e.g., in λ and HK97, respectively), this proposed trifunction protease/scaffold/capsid gene layout is a novel organization.

Cryoelectron microscopy reconstructions of Gifsy-2 capsids

Following induction and lysis, some "unfinished" particles (procapids, empty mature capsids, aberrant particles) are released from the bacterial host in addition to functional phage. After four subcultures, large amounts of these unfinished particles are obtained in solution. In samples purified by sucrose gradient, we observe by electron microscopy a majority of procapsids and a few expanded capsids (Fig. 3a). During storage at 4 °C, the proportion of expanded capsids to procapsids increases, from ~1:10 to ~1:4 after 4 weeks (Fig. 3c). Close inspection of the exterior edges of the expanded particles (Fig. 3c) reveals two kinds of particle: one with additional density on the outside (arrowed, and Fig. 3g) and one without (remaining expanded particles, and Fig. 3f). We note that partially decorated particles are not observed (see also the sections through the reconstructions, where occupancy of the decoration volume is either 0% (Fig. 5b) or 100% (Fig. 5c)), suggesting that one kind of particle is competent to bind decoration and the other is not. The bare particles are likely procapsids that expanded spontaneously, as happens for HK97 and T7, but in the absence of decoration molecules. We also noted a few procapsids with darker appearances (asterisk Figs. 3c, and d) that may represent unproteolyzed or partially proteolyzed procapsids, akin to the HK97 prohead I which is also darker in appearance than the proteolyzed prohead II (Conway et al., 1995). However, these were few in number although sufficient for an initial structural analysis. In total, we have 4 different capsid forms in solution: dark procapsid, procapsid, expanded procapsid, and empty mature capsid. Structures of these have been determined by cryoelectron microscopy and image analysis (see Table 1 for details). All the capsid forms exhibit icosahedral symmetry with a triangulation number T = 7 as is common for λ-like bacteriophages, and the hand has been assigned as *laevo* to match the known structure for HK97 (Lata et al., 2000; Wikoff et al., 2000).

Procapsid reconstruction

The procapsid reconstruction achieved the highest resolution of this study—11.8 Å—due to the large dataset of particles from which 6200 images were included in the final map (Fig. 4a). The exterior surface reveals the typical T = 7 arrangement of pentamers at the vertices and hexamers elsewhere. The latter are skewed and respect nonimposed pseudo two-fold symmetry, as for HK97 (Conway et al.,

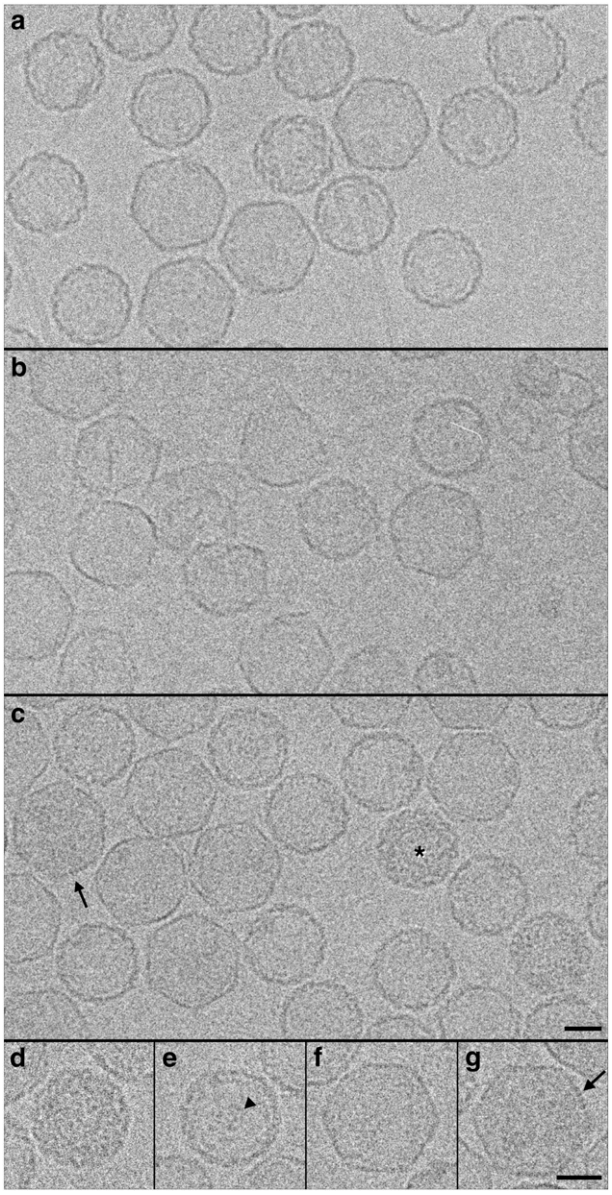

Fig. 3. Induced and purified phage particles imaged by cryoEM as (a) a freshly prepared sample, (b) after 2 weeks storage at 4 °C, and (c) 1 month later. Some expanded particles in (b) appear to have ruptured, and examples of darker particles are marked in (c) including a procapsid (asterisk) and mature capsid (arrow). Particles representative of various classes include (d) dark procapsid, possibly before proteolysis; (e) procapsid after proteolysis, for which the connector appears to be visible (arrowhead); (f) expanded procapsid; and (g) mature empty capsid with additional density indicated (arrow). Bars = 250 Å.

1995). The sectioned view of the interior surface emphasizes the highly contoured capsid wall that includes capsomer 'blisters' as well as clusters on the local 3-fold axes separated by distinct grooves at the 2-fold axes. These trimeric clusters appear to mediate contacts between capsomers. The central section (Fig. 5a, left) corresponding to the sectioning plane reveals pores in the capsid along the 5-fold and local 3-fold axes, indicating that the structure is not fully closed and would allow the exit of peptides (such as products of proteolysis), as proposed for the HK97 prohead (Conway et al., 1995).

Table 1
Details of reconstructions.

	Count of focal pairs	Count of particles extracted	Count of particles used	Estimated resolution (Å)
Procapsids (dark)	51	62	56	25.6
Procapsids	51	12 303	6200	11.8
Expanded procapsids	49	5266	3281	15.3
Empty mature capsids	49	2706	1090	16.7

The Gifsy-2 procapsid appears to be at the same stage along the assembly pathway as the Prohead II of HK97: proteolyzed and ready for packaging the DNA genome and for expanding. The trimmed lengths of the capsid proteins are 32 and 31 kDa for Gifsy-2 and HK97, respectively. In comparison with the HK97 prohead II structure, solved to a similar 12 Å resolution by cryoEM (Conway et al., 2001) and recently to atomic resolution by crystallography (Gertsman et al., 2009), the overall morphology of the Gifsy-2 procapsid is quite similar, including the skewed hexamers. Central sections side-by-side (Fig. 5a) show similar general features but differences in diameter (570 Å for Gifsy-2 and 470 Å for HK97) and degree of curvature in the region of the vertices.

Expanded procapsid reconstruction

The observation of spontaneous expansion among purified procapsids in storage buffer indicates that the procapsid is capable of embarking upon maturation. However, we expect that there are one or more intermediate states between procapsid and expanded procapsid (Lata et al., 2000) that could persist long enough to be represented in the micrographs and may affect achievable resolution. Images from 3281 particles were combined to calculate a density map of the expanded procapsid to 15.3 Å resolution. The surface views (Fig. 4b) show the large scale of the changes when compared to the procapsid. The general aspect is flatter than the procapsid—the capsid wall thickness is reduced from 44 to 30 Å while the diameter has increased to ~630 Å and the interior volume is larger by ~58%. As for HK97, the hexamers are no longer skewed after expansion and instead exhibit 6-fold symmetry or close to it. On the exterior surface, a continuous groove surrounds each hexamer and pentamer, appearing to delimit the boundary between capsomers, and the main intracapsomer contacts seem to be located at the 3-fold axis as for the procapsid but on the outside surface. Comparison of the central section with that from the atomic model of the HK97 mature capsid rendered at the same resolution (Fig. 5b) reveals a similar thickness for the capsid wall and similar overall shape, with Gifsy-2 being larger, less angular, and with more protrusions.

Empty mature capsid reconstruction

The empty mature capsid was less well represented on the cryoelectron micrographs than the expanded procapsid form of Gifsy-2 and was difficult to distinguish from the expanded procapsid. However, careful assignment of particles to one or the other class according to the presence of visible external density yielded quite distinct results. The exterior surface of the empty mature capsid, resolved to 16.7 Å (Fig. 4c), has the same organization of pentamers and hexamers as the other capsids as well as a shape and dimensions similar to the expanded procapsid. However, additional density is present at all sites of local 3-fold symmetry, consistent with the cryoEM images, and which represents a decoration molecule. By location, this molecule is analogous to gpD of phage λ (Dokland and Murialdo, 1993; Yang et al., 2000) and soc of phage T4 (Iwasaki et al., 2000), both of which form trimers, but its trefoil mushroom-like shape (Figs. 4c and 5c) more closely resembles the gpD trimer that is necessary for stabilization of the mature λ capsid and for packaging the full viral genome (Lander et al., 2008; Sternberg and Weisberg, 1977). The Gifsy-2 molecule is larger than λ's gpD, as visualized in the comparison of sections (Fig. 5c) and when modeled by the λ gpD trimer (see below). The interior surface of the Gifsy-2 mature capsid

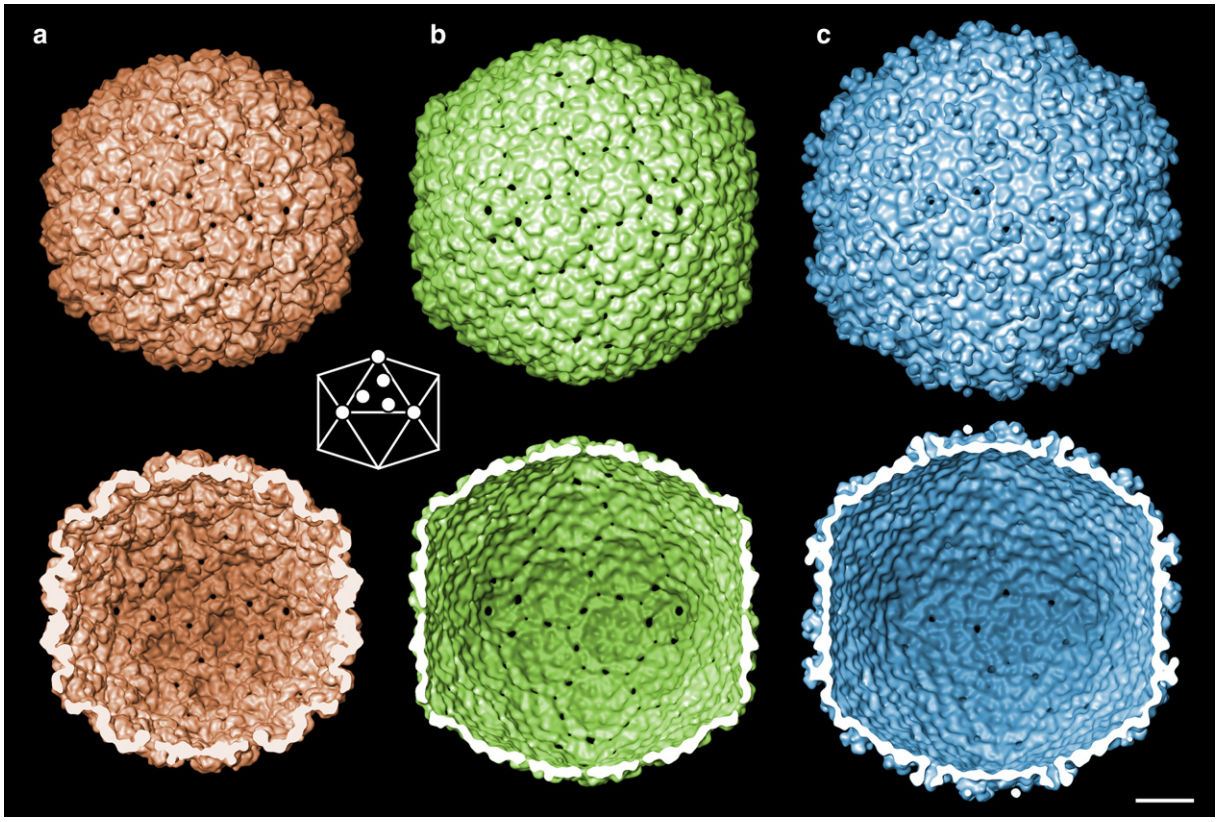

Fig. 4. Reconstructions from cryoEM data viewed along an icosahedral 2-fold axis: top row—exterior view; bottom row—inside view. (a) Gifsy-2 procapsid. (b) Expanded procapsid. (c) Mature empty capsid. Inset is a diagram of the capsomer positions corresponding to a lattice with T = 7*laevo* geometry. Bar = 100 Å.

(Fig. 4c) appears unchanged by binding of the decoration molecule compared to the expanded procapsid (Fig. 4b), suggesting that the contact is entirely on the outer surface. However, the estimated interior volume of the mature capsid is 7% larger than for the expanded procapsid, corresponding to a 2.2% increase (7.0 Å) in average radius, suggesting that binding of the decoration molecule may induce a small but measurable change in the capsid in addition to, or perhaps as a consequence of, 'cementing' capsid protein subunits together. Recent high-resolution structural work on analogous decoration proteins did not examine any effects their binding had on capsid structure (Lander et al., 2008; Qin et al., 2010).

Detailed mechanism of the binding of the minor capsid protein

Binding of the decoration protein on the Gifsy-2 capsid is revealed in more detail by comparing sections perpendicular to the binding site at the icosahedral 3-fold axis from the expanded procapsid and empty mature capsid as well as from a difference map calculated between them (Fig. 6). At a radius just beneath the exterior surface of the capsid (column A), no difference density is visible at the icosahedral 3-fold axis, although adjacent, obliquely sectioned trimer densities appear at the periphery of the sections. At the capsid surface (column B), three small spots, surrounded by the colorized hexamer densities,

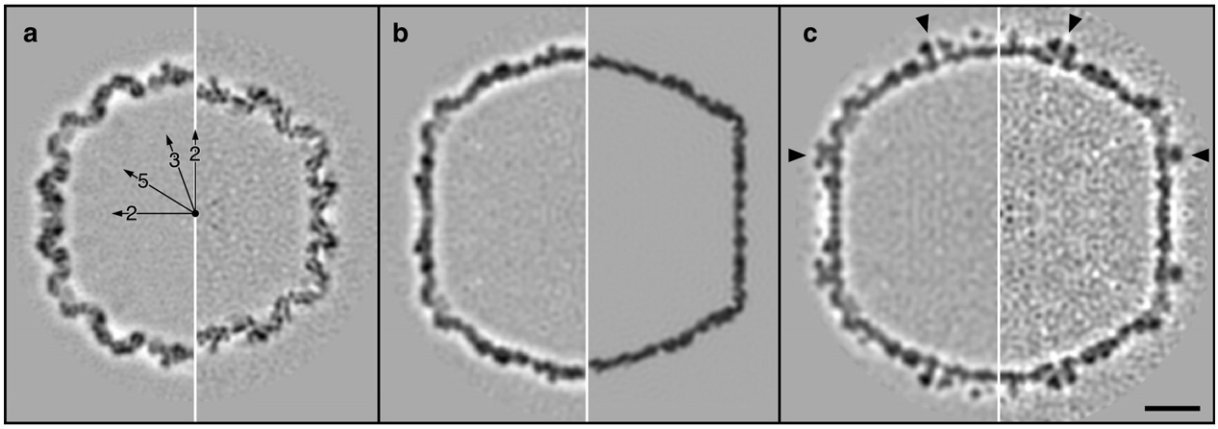

Fig. 5. Comparison of central sections: (a) Gifsy-2 procapsid (left) and HK97 prohead II at 12 Å (right) (Conway et al., 2001). (b) Gifsy-2 expanded procapsid (left) and HK97 atomic model of the mature capsid rendered at 15 Å (right). (c) Gifsy-2 mature empty capsid (left) and λ mature capsid at 17 Å (right) (Yang et al., 2000). Positions of symmetry axes are indicated in (a) and decoration density in Gifsy-2 and the corresponding gpD density in λ are indicated by arrowheads in (c). Bar = 100 Å.

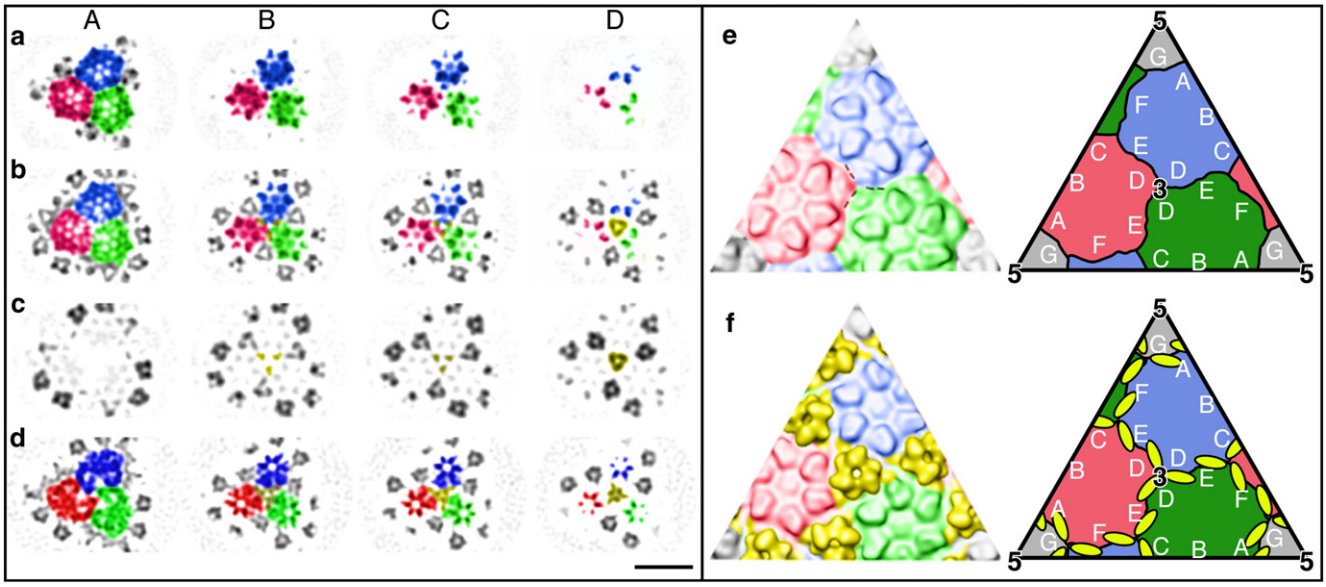

Fig. 6. Selected sections at increasing distances from the center (columns A–D) through the density maps of (a) the expanded procapsid, (b) mature empty capsid, and (c) the difference map between them, perpendicular to the icosahedral 3-fold axis. The blue, red, and green colors represent the density of the 3 hexamers of the major capsid protein adjacent to this axis. Density identified as the decoration molecule, according to the difference map, is colored yellow. (d) Below are corresponding sections from the mature capsid of phage λ (Yang et al., 2000) where the hexamer (gpE) and decoration (gpD) densities are similarly colored. Note the slight rotation of the gpD trimer and its less extensive "footprint" compared to that for Gifsy-2. Bar = 100 Å. Icosahedral facets of the rendered surfaces of the expanded procapsid (e) and mature empty capsid (f) viewed along an icosahedral 3-fold axis. Hexamers of the major capsid protein are colored in blue, green, and red, pentamers in gray, and the decoration molecules in yellow. The dashed lines in (e) represent the approximate position of the binding "footprint" of one decoration molecule on the surface. Schematic representations of the major capsid subunit locations are given at right, corresponding to the surfaces on the left and using the A–G numbering for HK97 (Conway et al., 2001). The yellow regions indicate the binding footprints of the decoration molecules, which appear to extend between adjacent copies of the major capsid protein from different hexamers towards a third copy.

indicate the onset of the central trimer, and these spots strengthen towards the radius of the hexamer tips (column C) and merge into a strong, trimeric blob just above the radius of the hexamers (column D). Contacts between the trimer and the underlying hexamers are evident in the empty mature capsid sections (columns B and C).

Correlation of the density sections and surface features allows us to distinguish subunit boundaries and propose a model for the pattern of interactions between the capsid and decoration proteins, as indicated schematically in Fig. 6. According to the numbering system for HK97 capsid protein subunits (Conway et al., 2001), D subunits from 3 hexamers approach at the icosahedral 3-fold axis but do not appear to have extensive contacts as there is a noticeable groove separating them in the expanded procapsid surface (Fig. 6e). The decoration molecule of the mature empty capsid (Fig. 6f—indicated in yellow) appears to contact the capsid surface in these grooves, each decoration subunit contacting two of the D subunits, and also extending away from the 3-fold axis towards an adjacent E subunit. This pattern is repeated at the local 3-fold sites with the local capsid subunits. In summary, the decoration molecule appears to contact as many as six capsid protein subunits, presumably to confer stability on the expanded Gifsy-2 capsid.

Localization of scaffold density

A small population of procapsids present a darker appearance (Fig. 3c) that suggests additional internal density, as would be expected for pre-proteolyzed procapsids such as the HK97 Prohead I (Conway et al., 1995). Images of 62 such particles were collected for analysis and 56 included in the final reconstruction resolved to 25.6 Å (Fig. 7). The most notable feature is inwardly directed density attached to the interior surface of the capsid, manifest as 5-lobed rings beneath the

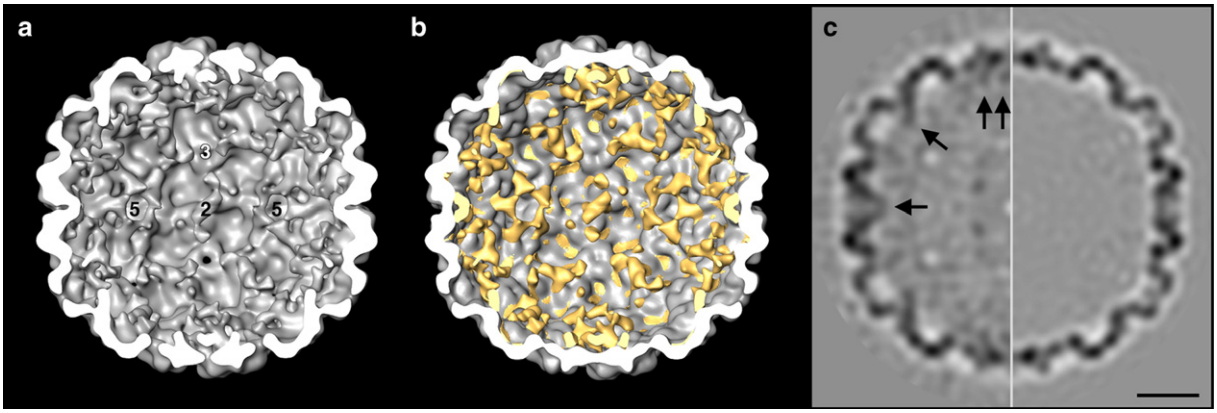

Fig. 7. Structural characterization of density internal to procapsids. (a) Surface representation of the reconstruction calculated from "darker" procapsids images (Fig. 3c) to 25.6 Å resolution. Positions of symmetry axes are marked. (b) Proteolyzed procapsid map (Fig. 4a) limited to the same 25.6 Å resolution (gray) and with the difference map between it and the "darker" procapsid map superimposed in a different color. (c) Central sections through the "darker" procapsid map, on the left, and the band-limited proteolyzed map, on the right. Arrows indicate strong additional density presumably due to scaffold proteins or the N-terminal of the capsid protein. Bar = 100 Å.

pentamers and arches between hexamers on the 2-fold icosahedral axis (Fig. 7b). As with the HK97 Prohead I, this density appears to be from the N-terminal portion of the full-length capsid protein and is more disordered the further it is away from the capsid. The central section (Fig. 7c) shows internal background that is considerably darker than for the proteolyzed procapsid, which would be consistent with an extensive but poorly structured N-terminal domain. While this pre-proteolyzed procapsid form is potentially the most interesting novel structure of Gifsy-2, the paucity of images likely limits to some degree the structural features resolved. Presumably, proteolysis occurs shortly after capsid assembly, and more details of the internal density may be revealed from particles assembled by expressing full-length capsid protein with the catalytic triad rendered nonfunctional by point mutation.

Structural comparison of Gifsy-2 with available atomic models

The mature HK97 capsid, solved crystallographically (Helgstrand et al., 2003; Wikoff et al., 2000), has been used successfully to model the major capsid proteins of phages T4 (Fokine et al., 2005) and phi29 (Morais et al., 2005) and fits very well into the cryoEM structures of phages P22 (Jiang et al., 2003), T5 (Effantin et al., 2006), T7 (Agirrezabala et al., 2007), ε15 (Jiang et al., 2008), and λ (Lander et al., 2008) despite low protein sequence homology. The HK97 gp5 fold may well represent a family utilized widely by phages and possibly some animal viruses (Duda et al., 2006; Steven et al., 2005). Given the apparent similarities in the ordering of structural genes as well as the capsid geometries shared by HK97 and Gifsy-2, we have attempted to dock the HK97 gp5 subunit atomic model into our density map of the mature capsid (Figs. 8a and b). Even at 16.7 Å resolution, the fit is visibly good for the core A and P domains of HK97 gp5, with most difference at the region of the P domain adjacent to the 3-fold axes (Fig. 8a). This may be expected as the Gifsy-2 capsid binds a decoration molecule here while HK97 does not. The remainder of HK97 gp5—the E-loop and N-terminal arm—does not fit well, and again, we may expect this because the functions of these regions are not expressed in the same manner for Gifsy-2. In particular, a residue

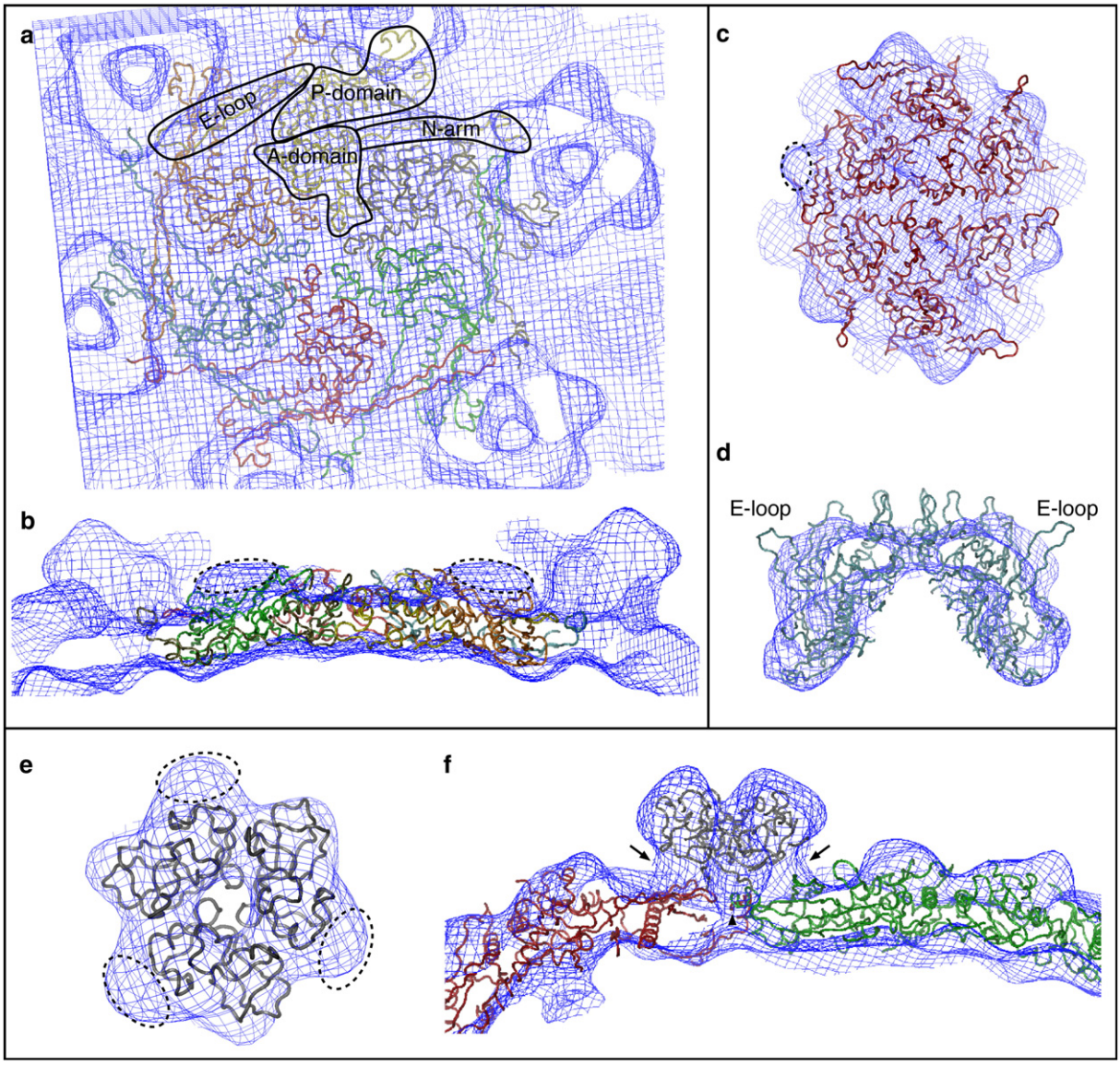

Fig. 8. Docking of atomic models into the Gifsy-2 density maps (blue mesh) with unoccupied regions of the cryoEM density map indicated with ovals. Views of the mature HK97 capsid protein hexamer (PDB 1OHG) docked into the Gifsy-2 empty mature capsid from the top (a), and side (b). The four different domains of the HK97 gp5 subunit are indicated in (a). Docking of the pseudo-atomic model of HK97 procapsid (PDB 1IF0) into the Gifsy-2 cryoEM density is shown as a top view (c) and side view (d) where the HK97 gp5 E-loop protruding from the cryoEM envelope is indicated. Fit of the phage λ gpD decoration molecule (PDB 1C5E; colored gray) into the mature empty capsid is shown from the top (e) and side (f), which also includes the HK97 gp5 models for hexamers. At the 3-fold axis, the N-terminal arms (arrowhead) of the gp5 models clash, and density at the base of the Gifsy-2 decoration are not fit by the truncated gpD molecule, as indicated with arrows.

at the tip of the HK97 E-loop is cross-linked to a neighboring subunit and no such cross-link is evident for Gifsy-2. This cross-link is most likely a stabilizing mechanism that is an alternative to binding decoration molecules. A region of unoccupied density in the Gifsy-2 map (ovals in Fig. 8b) is adjacent to the HK97 gp5 E-loops, and we suppose that the Gifsy-2 capsid protein is folded differently from the E-loop so as to fill this region. The proteolyzed Gifsy-2 capsid protein is also approximately 10 residues longer than for HK97, and these residues may also contribute to the unoccupied volume.

We have also fit the HK97 gp5 subunit from a pseudo-atomic resolution structure of the HK97 procapsid (Conway et al., 2001) into our density map of the Gifsy-2 procapsid (Figs. 8c and d). Most observations for the empty mature capsid fitting also apply here, despite the ~40 Å and ~40° tumbling of the HK97 gp5 subunits from their positions in the mature capsid. As before, the E-loop noticeably extends outside the Gifsy-2 density map and an unoccupied region of density is adjacent to it. The two procapsid maps differ more by size than the mature capsid maps do and our modeling indicates that the differences are principally in curvature of the capsid and in the pentamer, which is wider for Gifsy-2 than for HK97 (Fig. 8d). These differences precluded our docking the HK97 asymmetric unit directly into the Gifsy-2 procapsid, and instead, we modeled the procapsid with the HK97 gp5 hexamer and a pentamer subunit allowing some freedom of movement for the latter.

The decoration density was also modeled by fitting the atomic model of the λ gpD trimer (Yang et al., 2000) into the Gifsy-2 empty mature capsid (Figs. 8e and f). The gpD molecule follows the shape of the Gifsy-2 density very well, especially the lobes that give the strong trimeric appearance, although it is clearly smaller leaving some unoccupied density at the top of the Gifsy-2 mushroom, corresponding to ~15 residues per monomer, and also at the base. As the gpD crystal structure lacked the amino-terminal 14 residues, which interface with the capsid surface, the poor fit at the base is expected, and combined with the poor fit for the adjacent major capsid subunit density, modeling of the decoration–capsid interface was not possible. However, based on comparison with sections through the mature λ capsid reconstruction (Fig. 6) and modeling based on a more recent subnanometer reconstruction of the mature λ capsid (Lander et al., 2008), the Gifsy-2 decoration molecule appears to follow a similar pattern of interactions with the underlying capsid protein as for phage λ. Generally, the morphological evidence strongly supports assignment of the Gifsy-2 decoration molecule as an analog of λ gpD that assembles as a trimer of a similarly sized protein.

Discussion

Several lambdoid phage capsids have been solved to moderate resolution by cryoEM, including λ (Dokland and Murialdo, 1993; Lander et al., 2008; Yang et al., 2000), P22 (Jiang et al., 2003; Zhang et al., 2000), (Jiang et al., 2008), and T7 (Agirrezabala et al., 2005; Cerritelli et al., 2003), and one—HK97—has been solved crystallographically (Helgstrand et al., 2003; Wikoff et al., 2000). Other capsids with closely related structural features include T5 (Effantin et al., 2006), phi29 (Morais et al., 2005), and T4 (Fokine et al., 2004; Fokine et al., 2005). These capsids generally assemble as a precursor expressing asymmetric hexons but expand into a thin-walled polyhedral capsid with hexon asymmetry cured. The capsid morphologies and underlying folds have much in common with the HK97 capsid, and the gp5 capsid protein fold has been observed to date in the major capsid proteins of T4, phi29, λ, and ε15. Lower-resolution structures of other icosahedral capsids are consistent with the HK97 fold, including that of herpesvirus (Baker et al., 2005). Gifsy-2 does not depart from this pattern but adds a new variation in which the coding sequences of three genes, protease, scaffolding, and major capsid protein, have been fused into one gene encoding the three protein functions. The good fitting of the core HK97 gp5 domains suggests that the Gifsy-2 capsid likely has the HK97 fold, despite low sequence homology, and similarly its decoration molecule appears to be a close structural analog of λ's gpD. This mixture of structural features is a reflection of the mosaicity of phage genomes in general. Furthermore, the unique fusion of capsid protein functions into a single open reading frame appears also to be a combination of the strategies used by HK97 and λ and would be expected to have consequences in the assembly pathway, as discussed below.

One of the unique aspects of Gifsy-2 is the long capsid protein gene that includes three regions: the N-terminal ClpP protease-like domain, a central domain of unknown function, and the C-terminal mature capsid protein as established by N-terminal sequencing of assembled particles. It is tempting to speculate that the central domain performs a scaffolding role, similar to that proposed for the N-terminal 102 residues of the HK97 gp5 capsid protein and the N-terminal 159 residues of the T5 gp8 capsid protein, and that the viral protease removes itself and this domain after assembly of the first procapsid form. However, as yet little direct evidence supports this proposal other than the visualization of "dark" procapsids that conceivably retain some unproteolyzed full-length capsid protein. N-terminal sequencing was not definitive on this point as the vast majority of particles were proteolyzed and the evidence already removed. A distinctive feature predicted for the HK97 and T5 N-terminal domains is a high proportion of coiled coil, but in the Gifsy-2 central region, we see only a very modest prediction. However, the λ scaffold, coencoded on the gpC/Nu3 gene with the protease, likewise has no remarkable prediction for coiled coil structure. Nonetheless, Gifsy-2 appears to combine features of HK97 and λ to produce a unique assembly strategy—combined protease-scaffold that is covalently linked to the capsid protein. Future work will include expressing mutants of the long capsid protein gene with the ClpP protease catalytic residues replaced, aiming to assemble large quantities of particles corresponding to the unproteolyzed HK97 prohead I with which N-terminal sequencing and structural work will characterize the extent and organization of the capsid protein domains.

Both the interior and exterior surfaces of the Gifsy-2 capsid appear to have special features related to the local and icosahedral three-fold sites. The protruding trimer clusters on the inside of the Gifsy-2 procapsid are more marked than for the HK97 prohead II and bear some resemblance to the 'nubbins' of density observed on the interior of the T7 procapsid that may be remnants of the gp9 scaffold protein (Cerritelli et al., 2003). The internal 3-fold sites of the phage P22 capsid are also involved in interactions with scaffold proteins (Thuman-Commike et al., 1998, 1999a). Preliminary analysis of the few Gifsy-2 "dark" procapsids revealed additional density continuous with the internal local 3-fold sites that is likely to be scaffolding and follows the T7 and P22 binding patterns. We conclude that the trimer clusters we observe in the Gifsy-2 procapsid reconstruction most probably includes the post-proteolytic N-terminal of the mature capsid protein.

Supplementary proteins that bind as trimers to the external 3-fold sites and stabilize the mature form of the viral capsid have been observed for other phages, including T4's soc (Iwasaki et al., 2000; Olson et al., 2001) and λ's gpD (Dokland and Murialdo, 1993). The T4 soc molecule binds around the hexamers (but not the pentamers) forming continuous rings (Qin et al., 2010), unlike the more 3-fold localized mushrooms observed for Gifsy-2 and λ (Lander et al., 2008; Yang et al., 2000). The differences in shape and in contact area with the capsid likely reflect different structural requirements between the larger T4 capsids and the T = 7 lambdoid phages. Although the Gifsy-2 decoration molecule has a similar trimeric shape to the λ gpD trimer, it has extra density located near the corresponding C-terminal of each gpD monomer (see Fig. 8) suggesting a longer protein. The sequence of the Gifsy-2 molecule remains to be determined, but since no part of the Gifsy-2 genome scores any significant homology with λ gpD, the two proteins are clearly unalike at this level despite structural similarity, much as for viral capsid proteins in general.

The λ gpD molecules are essential for packaging of the complete λ genome (Sternberg and Weisberg, 1977) and will bind gpD capsids (analog to the Gifsy-2 expanded procapsid) but not to procapsids (Imber et al., 1980). This suggests that the accessory protein is necessary for accommodating the high internal pressure of the packaged DNA (Kindt et al., 2001) but expansion is required to establish the binding site (Lander et al., 2008). We suppose that the Gifsy-2 molecule has the same function and binding pathway, and likely, a similar organization with the N-termini extended along the capsid surface, contacting 2 subunits beyond those adjacent to the 3-fold site.

Conclusions

We have established that the unique gene organization for the structural elements of the phage Gifsy-2 capsid yield a recognizably lambdoid shape, and the work on purified phage preparations described here will be the forerunner of efforts to express mutants that yield precursor nonproteolyzed capsids and to establish the decoration protein gene and its sequence. The function of the central domain encoded by the long capsid protein gene also remains to be established along with the arrangement of the N-terminal domains within the precursor capsid. Understanding the novel features of Gifsy-2 is likely to provide new insights into capsid assembly and the controls that produce different specific geometries from rather uniform structural units.

Materials and methods

Bacterial strains

Two different strains of *Salmonella typhimurium* ATCC14028 were used to produce bacteriophages. Gifsy-2 phage was induced in the donor strain, MA7599 (Gifsy-1[−]/Gifsy-2[+]/Gifsy-3[−]), to a concentration of 10^4 ph/mL after overnight incubation in LB at 30 °C. Amplification of Gifsy-2 was done by the recipient strain, MA6710 (Gifsy-1[−]/Gifsy-2[−]/Gifsy-3[−]), also cultured overnight in LB at 30 °C without shaking. Unless specified, the buffer used for dilution, pellet suspension, and sucrose gradient is a λ-dilution like buffer (10 mM Tris–HCl pH 7.5, 10 mM $MgSO_4$; Dokland and Murialdo, 1993). The two strains were cured of phages Gifsy-1 and Gifsy-3 to avoid contamination as these have been shown to grow more easily than Gifsy-2 (Figueroa-Bossi and Bossi, 1999).

Capsid preparation

Gifsy-2 procapsids, expanded procapsids, and empty matured capsids were obtained as follows. First, after an overnight culture of both strains MA7599 and MA6710 (10^9 bacteria/mL), 100 μL of the supernatant of MA7599 (9000 rpm, 5-10 min) were mixed with 100 μL of the 10^{-4} dilution of MA6710 (MOI = 1) in 2.5 mL of LB. To improve the phage titer (10^7 ph/mL), the same mixing was repeated at an MOI = 1 with 100 μL of the supernatant of MA7599 and 100 μL of the 10^{-2} dilution of MA6710. The phage mixture was then subcultured at the same MOI in 30 mL of LB (1.5 mL of MA7599 supernatant with 150 μL of MA6710) and finally in 1 L of LB (30 mL of MA7599 supernatant with 15 mL of MA6710). The last lysate was purified essentially as described (Yamamoto et al., 1970). First, it was treated with DNAase (1 μg/mL) for 30 min at room temperature with shaking. NaCl was added to a final concentration of 1 M with shaking and left on ice for 1 h. Cells debris was removed by centrifugation at 8500 rpm, 25–30 min (Beckman JA-10) until the supernatant clarified. The phage particles were directly pelleted by centrifugation at 18000 rpm for 2 h (Beckman JA-20) or subjected to an overnight precipitation (at 4 °C) by addition of PEG8000 (10% wt./vol.) followed by pelleting at 8500 rpm, 30–40 min (JA-10). For both methods, the pellets and the precipitated material were gently suspended in fresh buffer overnight at 4 °C. The crude sample of particles was sometimes concentrated by ultracentrifugation on a TLS-55 rotor (30000 rpm, 2 h) to obtain sufficient material for loading on top of a 15–30% sucrose gradient (Thuman-Commike et al., 1999b) which was centrifuged at 25000 rpm for 4 h on a SW40 rotor. The most pure fractions of 1 mL were identified by SDS-PAGE as well as direct visualization by negative-stain electron microscopy. The rejected impure material from the first sucrose gradient was reloaded onto a fresh sucrose gradient. The purified Gifsy-2 particles (essentially procapsids) were pooled together, dialyzed against a new buffer (50 mM Tris–HCl (pH = 7.6), 100 mM $MgCl_2$) for storage and concentrated with a Centricon 100 kDa filter (Millipore). A 5-fold dilution was assayed for purity by negative stain EM before imaging by cryoEM.

Electron microscopy

Samples were prepared for negative-stain EM by pipetting ~2 μL of sample between a sheet of mica and a film of evaporated carbon, floating the carbon film off in a pool of negative stain (uranyl acetate for procapsids or ammonium molybdate for heads), placing a copper EM grid on the floating film, and picking this up with a particularly absorbent type of newspaper. The grid carbon sample sandwich was placed on filter paper to blot and air-dry for at least 10 min before insertion into the column of a JEOL JEM 1200EX II microscope equipped with a tungsten filament and operating at 100 kV.

Cryoelectron microscopy was performed according to a standard procedure (Cheng et al., 1999). Briefly, ~2 μL of purified sample at a concentration of 0.5–1 mg/ml was pipetted onto a copper grid covered by a thin holey carbon film. Excess liquid was removed by a brief blotting before plunge freezing the grid into liquid ethane cooled by a liquid nitrogen bath. Frozen grids were transferred to a Gatan 626 cryoholder and inserted into an FEI CM200 with a LaB_6 filament operating at 200 kV, maintaining liquid nitrogen temperature throughout. Images were and taken at a nominal magnification of 38,000×. For each selected area, image pairs were taken within a range of defocus of −1 to −4 μm.

Three-dimensional image analysis

Negatives were screened for particle appearance and overlap, thickness and quality of ice, apparent defocus (contrast), and drift. Fifty-one image pairs were selected and scanned on a Z/I Photoscan (previously called the Zeiss SCAI) at a step size of 7 μm corresponding to 1.84 Å/pixel at the sample. Image analysis followed an established method (Conway and Steven, 1999) but starting from reconstructions calculated from negative-stain images (Effantin et al., 2006). Resolution estimation was done by calculating the Fourier shell correlation (Saxton and Baumeister, 1982) between independent half-data set density maps and applying a cutoff at a correlation coefficient of 0.3 (see Supplementary data). Details of the reconstructions are listed in Table 1. All analyses were run on PowerMac G5 computers (Apple Computer, Cupertino, CA, USA), and surface views of reconstructions were generated with Amira (Mercury Computer Systems/3D Viz group, San Diego, CA, USA, and Merignac, France) running on Linux workstations (Dell, Austin, TX, USA).

Images of expanded procapsids and mature empty capsids, being visually similar, were treated together during the first part of the analysis. The numerical dominance of expanded procapsids led to a solution that excluded the mature empty capsids. These excluded images were then refined independently to give the density map for the mature empty capsid of Gifsy-2. Density maps are deposited in the EBI database with accession numbers as follows: procapsid: EMD-1691; dark procapsid: EMD-1692; expanded procapsid: EMD-1693; and empty mature capsid: EMD-1694.

SDS–polyacrylamide gel analysis and amino-terminal protein sequencing

Precast gels (15% acrylamide, 12 wells, 20 μL/well) from Bio-Rad were run on a Mini-PROTEAN 3 cell (Bio-Rad) under conditions specified by the manufacturer that corresponded essentially to the standard method as originally described (Laemmli, 1970). Transfer of the protein bands onto PVDF membrane (Millipore Immobilon PSQ) was done at room temperature in a standard CAPS buffer (10 mM CAPS, pH 11, 10% vol./vol. methanol) for 2 h at 50 V. Staining was done for 1 min in 0.1% Coomassie blue, 1% acetic acid, and 40% methanol, and destaining in 50% methanol until bands appeared clearly (5–10 min). Amino acid sequence determination based on Edman degradation was done on an Applied Biosystems gas-phase sequencer model 492.

Amino acid sequence analysis

Sequence alignment of Gifsy-2 gene product that includes the capsid protein was generated using ClustalW (Thompson, Higgins and Gibson, 1994) as available from the EMBL-EBI Web site http://www.ebi.ac.uk/clustalw. Assignment of the C-terminal major capsid protein function to the same gene product from the N-terminal sequencing result and sequence similarities was done using the program BLAST (Altschul et al., 1997) at the NIH-NCBI Web site http://www.ncbi.nlm.nih.gov/BLAST/.

Docking of atomic subunits in Gifsy-2 density maps

The pseudo-atomic model of the HK97 procapsid (Conway et al., 2001) and atomic models of the HK97 mature capsid (Helgstrand et al., 2003; Wikoff et al., 2000) and the λ gpD trimer (Yang et al., 2000) were obtained from the PDB (http://www.rcsb.org/pdb/) with IDs of 1IF0, 1OHG, and 1C5E, respectively. Initially the atomic models were manually fit into Gifsy-2 density maps using O (Jones et al., 1991). All subsequent docking procedures were carried out using the SITUS package (Wriggers and Birmanns, 2001) and particularly the CoLoRes module for rigid-body docking (Chacon and Wriggers, 2002). Electron density maps were first truncated to the zone of interest. Visualization of the docking results was done with the VMD package (Humphrey et al., 1996) available at http://www.ks.uiuc.edu/Research/vmd/.

Acknowledgments

The authors wish to thank Dr Jean Lepault for proposing and encouraging this project and Drs S.R. Casjens, R.W. Hendrix, R.L Duda, and A.C. Steven for helpful discussions and advice and together with Dr. R.H. Wade for support. The authors are grateful to J. P. Andrieu for aid with N-terminal sequencing and to Drs D.M. Belnap, B. Heymann, and T.S. Baker for kindly aiding with the 3D analysis software. Dr R.H. Ruigrok provided access to his JEOL 1200EX microscope, and expert technical assistance in cryoEM by Drs E. Neumann and E.A. Hewat and in computational support by Dr. F. Metoz is gratefully recognized. Drs B. Delmas and C. Chevalier are thanked for help with the sucrose gradient step of particle purification. The cryoEM reconstruction of phage λ was provided by Drs. A.C. Steven and N. Cheng. Support is acknowledged by J.F.C. from the French CNRS in the form of an ATIP grant and the Commonwealth of Pennsylvania (SAP 4100031302).

Appendix A. Supplementary data

Supplementary data associated with this article can be found, in the online version, at doi:10.1016/j.virol.2010.03.041.

References

Agirrezabala, X., Martin-Benito, J., Caston, J.R., Miranda, R., Valpuesta, J.M., Carrascosa, J.L., 2005. Maturation of phage T7 involves structural modification of both shell and inner core components. Embo J 24 (21), 3820–3829.
Agirrezabala, X., Velazquez-Muriel, J.A., Gomez-Puertas, P., Scheres, S.H., Carazo, J.M., Carrascosa, J.L., 2007. Quasi-atomic model of bacteriophage t7 procapsid shell: insights into the structure and evolution of a basic fold. Structure 15 (4), 461–472.
Altschul, S.F., Madden, T.L., Schaffer, A.A., Zhang, J., Zhang, Z., Miller, W., Lipman, D.J., 1997. Gapped BLAST and PSI-BLAST: a new generation of protein database search programs. Nucleic Acids Res. 25 (17), 3389–3402.
Baker, M.L., Jiang, W., Rixon, F.J., Chiu, W., 2005. Common ancestry of herpesviruses and tailed DNA bacteriophages. J Virol 79 (23), 14967–14970.
Bamford, D.H., Grimes, J.M., Stuart, D.I., 2005. What does structure tell us about virus evolution? Curr. Opin. Struct. Biol. 15 (6), 655–663.
Cardarelli, L., Lam, R., Tuite, A., Baker, L.A., Sadowski, P.D., Radford, D.R., Rubinstein, J.L., Battaile, K.P., Chirgadze, N., Maxwell, K.L., Davidson, A.R., 2010. The crystal structure of bacteriophage HK97 gp6: defining a large family of head-tail connector proteins. J Mol Biol 395 (4), 754–768.
Cerritelli, M.E., Conway, J.F., Cheng, N., Trus, B.L., Steven, A.C., 2003. Molecular mechanisms in bacteriophage T7 procapsid assembly, maturation, and DNA containment. Adv. Protein Chem. 64, 301–323.
Chacon, P., Wriggers, W., 2002. Multi-resolution contour-based fitting of macromolecular structures. J Mol Biol 317 (3), 375–384.
Cheng, N., Conway, J.F., Watts, N.R., Hainfeld, J.F., Joshi, V., Powell, R.D., Stahl, S.J., Wingfield, P.E., Steven, A.C., 1999. Tetrairidium, a four-atom cluster, is readily visible as a density label in three-dimensional cryo-EM maps of proteins at 10–25 Å resolution. J Struct Biol 127 (2), 169–176.
Cheng, H., Shen, N., Pei, J., Grishin, N.V., 2004. Double-stranded DNA bacteriophage prohead protease is homologous to herpesvirus protease. Protein Sci. 13 (8), 2260–2269.
Conway, J.F., Steven, A.C., 1999. Methods for reconstructing density maps of "single" particles from cryoelectron micrographs to subnanometer resolution. J Struct Biol 128 (1), 106–118.
Conway, J.F., Duda, R.L., Cheng, N., Hendrix, R.W., Steven, A.C., 1995. Proteolytic and conformational control of virus capsid maturation: the bacteriophage HK97 system. J Mol Biol 253 (1), 86–99.
Conway, J.F., Wikoff, W.R., Cheng, N., Duda, R.L., Hendrix, R.W., Johnson, J.E., Steven, A.C., 2001. Virus maturation involving large subunit rotations and local refolding. Science 292 (5517), 744–748.
Dokland, T., Murialdo, H., 1993. Structural transitions during maturation of bacteriophage lambda capsids. J Mol Biol 233 (4), 682–694.
Duda, R.L., 1998. Protein chainmail: catenated protein in viral capsids. Cell 94 (1), 55–60.
Duda, R.L., Martincic, K., Hendrix, R.W., 1995. Genetic basis of bacteriophage HK97 prohead assembly. J Mol Biol 247 (4), 636–647.
Duda, R.L., Hendrix, R.W., Huang, W.M., Conway, J.F., 2006. Shared architecture of bacteriophage SPO1 and herpesvirus capsids. Curr. Biol. 16 (1), R11–R13.
Effantin, G., Boulanger, P., Neumann, E., Letellier, L., Conway, J.F., 2006. Bacteriophage T5 structure reveals similarities with HK97 and T4 suggesting evolutionary relationships. J Mol Biol 361 (5), 993–1002.
Figueroa-Bossi, N., Bossi, L., 1999. Inducible prophages contribute to *Salmonella* virulence in mice. Mol. Microbiol. 33 (1), 167–176.
Figueroa-Bossi, N., Coissac, E., Netter, P., Bossi, L., 1997. Unsuspected prophage-like elements in *Salmonella typhimurium*. Mol. Microbiol. 25 (1), 161–173.
Figueroa-Bossi, N., Uzzau, S., Maloriol, D., Bossi, L., 2001. Variable assortment of prophages provides a transferable repertoire of pathogenic determinants in *Salmonella*. Mol. Microbiol. 39 (2), 260–271.
Fokine, A., Chipman, P.R., Leiman, P.G., Mesyanzhinov, V.V., Rao, V.B., Rossmann, M.G., 2004. Molecular architecture of the prolate head of bacteriophage T4. Proc Natl Acad Sci U S A 101 (16), 6003–6008.
Fokine, A., Leiman, P.G., Shneider, M.M., Ahvazi, B., Boeshans, K.M., Steven, A.C., Black, L.W., Mesyanzhinov, V.V., Rossmann, M.G., 2005. Structural and functional similarities between the capsid proteins of bacteriophages T4 and HK97 point to a common ancestry. Proc Natl Acad Sci U S A 102 (20), 7163–7168.
Gertsman, I., Gan, L., Guttman, M., Lee, K., Speir, J.A., Duda, R.L., Hendrix, R.W., Komives, E.A., Johnson, J.E., 2009. An unexpected twist in viral capsid maturation. Nature 458 (7238), 646–650.
Helgstrand, C., Wikoff, W.R., Duda, R.L., Hendrix, R.W., Johnson, J.E., Liljas, L., 2003. The refined structure of a protein catenane: the HK97 bacteriophage capsid at 3.44 Å resolution. J Mol Biol 334 (5), 885–899.
Hendrix, R.W., 2002. Bacteriophages: evolution of the majority. Theor. Popul. Biol. 61 (4), 471–480.
Hendrix, R.W., Casjens, S., 2006. Bacteriophage lambda and its genetic neighborhood. 2nd ed. In: Abedon, S.T., Calendar, R.L. (Eds.), The Bacteriophages. Oxford University Press, New York.
Hendrix, R.W., Duda, R.L., 1998. Bacteriophage HK97 head assembly: a protein ballet. Adv. Virus Res. 50, 235–288.
Humphrey, W., Dalke, A., Schulten, K., 1996. VMD: visual molecular dynamics. J Mol Graph 14 (1), 33–38.
Imber, R., Tsugita, A., Wurtz, M., Hohn, T., 1980. Outer surface protein of bacteriophage lambda. J Mol Biol 139 (3), 277–295.
Iwasaki, K., Trus, B.L., Wingfield, P.T., Cheng, N., Campusano, G., Rao, V.B., Steven, A.C., 2000. Molecular architecture of bacteriophage T4 capsid: vertex structure and bimodal binding of the stabilizing accessory protein, Soc. Virology 271 (2), 321–333.
Jiang, W., Li, Z., Zhang, Z., Baker, M.L., Prevelige Jr., P.E., Chiu, W., 2003. Coat protein fold and maturation transition of bacteriophage P22 seen at subnanometer resolutions. Nat. Struct. Biol. 10 (2), 131–135.

Jiang, W., Baker, M.L., Jakana, J., Weigele, P.R., King, J., Chiu, W., 2008. Backbone structure of the infectious epsilon15 virus capsid revealed by electron cryomicroscopy. Nature 451 (7182), 1130–1134.

Jones, T.A., Zou, J.Y., Cowan, S.W., Kjeldgaard, 1991. Improved methods for building protein models in electron density maps and the location of errors in these models. Acta Crystallogr. A 47 (Pt 2), 110–119.

Kindt, J., Tzlil, S., Ben-Shaul, A., Gelbart, W.M., 2001. DNA packaging and ejection forces in bacteriophage. Proc Natl Acad Sci U S A 98 (24), 13671–13674.

Laemmli, U.K., 1970. Cleavage of structural proteins during the assembly of the head of bacteriophage T4. Nature 227 (5259), 680–685.

Lander, G.C., Tang, L., Casjens, S.R., Gilcrease, E.B., Prevelige, P., Poliakov, A., Potter, C.S., Carragher, B., Johnson, J.E., 2006. The structure of an infectious P22 virion shows the signal for headful DNA packaging. Science 312 (5781), 1791–1795.

Lander, G.C., Evilevitch, A., Jeembaeva, M., Potter, C.S., Carragher, B., Johnson, J.E., 2008. Bacteriophage lambda stabilization by auxiliary protein gpD: timing, location, and mechanism of attachment determined by cryo-EM. Structure 16 (9), 1399–1406.

Lata, R., Conway, J.F., Cheng, N., Duda, R.L., Hendrix, R.W., Wikoff, W.R., Johnson, J.E., Tsuruta, H., Steven, A.C., 2000. Maturation dynamics of a viral capsid: visualization of transitional intermediate states. Cell 100 (2), 253–263.

Morais, M.C., Choi, K.H., Koti, J.S., Chipman, P.R., Anderson, D.L., Rossmann, M.G., 2005. Conservation of the capsid structure in tailed dsDNA bacteriophages: the pseudoatomic structure of phi29. Mol Cell 18 (2), 149–159.

Morgan, G.J., Hatfull, G.F., Casjens, S., Hendrix, R.W., 2002. Bacteriophage Mu genome sequence: analysis and comparison with Mu-like prophages in *Haemophilus*, *Neisseria* and *Deinococcus*. J Mol Biol 317 (3), 337–359.

Olson, N.H., Gingery, M., Eiserling, F.A., Baker, T.S., 2001. The structure of isometric capsids of bacteriophage T4. Virology 279 (2), 385–391.

Qin, L., Fokine, A., O'Donnell, E., Rao, V.B., Rossmann, M.G., 2010. Structure of the small outer capsid protein, Soc: a clamp for stabilizing capsids of T4-like phages. J Mol Biol 395 (4), 728–741.

Ross, P.D., Conway, J.F., Cheng, N., Dierkes, L., Firek, B.A., Hendrix, R.W., Steven, A.C., Duda, R.L., 2006. A free energy cascade with locks drives assembly and maturation of bacteriophage HK97 capsid. J Mol Biol 364 (3), 512–525.

Saxton, W.O., Baumeister, W., 1982. The correlation averaging of a regularly arranged bacterial cell envelope protein. J. Microsc. 127, 127–138.

Shaw, J.E., Murialdo, H., 1980. Morphogenetic genes C and Nu3 overlap in bacteriophage lambda. Nature 283 (5742), 30–35.

Sternberg, N., Weisberg, R., 1977. Packaging of coliphage lambda DNA, II. The role of the gene D protein. J Mol Biol 117 (3), 733–759.

Steven, A.C., Heymann, J.B., Cheng, N., Trus, B.L., Conway, J.F., 2005. Virus maturation: dynamics and mechanism of a stabilizing structural transition that leads to infectivity. Curr. Opin. Struct. Biol. 15 (2), 227–236.

Thompson, J.D., Higgins, D.G., Gibson, T.J., 1994. CLUSTAL W: improving the sensitivity of progressive multiple sequence alignment through sequence weighting, position-specific gap penalties and weight matrix choice. Nucleic Acids Res. 22 (22), 4673–4680.

Thomson, N., Baker, S., Pickard, D., Fookes, M., Anjum, M., Hamlin, N., Wain, J., House, D., Bhutta, Z., Chan, K., Falkow, S., Parkhill, J., Woodward, M., Ivens, A., Dougan, G., 2004. The role of prophage-like elements in the diversity of *Salmonella enterica* serovars. J Mol Biol 339 (2), 279–300.

Thuman-Commike, P.A., Greene, B., Malinski, J.A., King, J., Chiu, W., 1998. Role of the scaffolding protein in P22 procapsid size determination suggested by T = 4 and T = 7 procapsid structures. Biophys. J. 74 (1), 559–568.

Thuman-Commike, P.A., Greene, B., Malinski, J.A., Burbea, M., McGough, A., Chiu, W., Prevelige Jr., P.E., 1999a. Mechanism of scaffolding-directed virus assembly suggested by comparison of scaffolding-containing and scaffolding-lacking P22 procapsids. Biophys. J. 76 (6), 3267–3277.

Thuman-Commike, P.A., Tsuruta, H., Greene, B., Prevelige Jr., P.E., King, J., Chiu, W., 1999b. Solution x-ray scattering-based estimation of electron cryomicroscopy imaging parameters for reconstruction of virus particles. Biophys. J. 76 (4), 2249–2261.

Wang, J., Hartling, J.A., Flanagan, J.M., 1997. The structure of ClpP at 2.3 Å resolution suggests a model for ATP-dependent proteolysis. Cell 91 (4), 447–456.

Wikoff, W.R., Liljas, L., Duda, R.L., Tsuruta, H., Hendrix, R.W., Johnson, J.E., 2000. Topologically linked protein rings in the bacteriophage HK97 capsid. Science 289 (5487), 2129–2133.

Wriggers, W., Birmanns, S., 2001. Using situs for flexible and rigid-body fitting of multiresolution single-molecule data. J Struct Biol 133 (2–3), 193–202.

Yamamoto, K.R., Alberts, B.M., Benzinger, R., Lawhorne, L., Treiber, G., 1970. Rapid bacteriophage sedimentation in the presence of polyethylene glycol and its application to large-scale virus purification. Virology 40 (3), 734–744.

Yang, F., Forrer, P., Dauter, Z., Conway, J.F., Cheng, N., Cerritelli, M.E., Steven, A.C., Pluckthun, A., Wlodawer, A., 2000. Novel fold and capsid-binding properties of the lambda-phage display platform protein gpD. Nat. Struct. Biol. 7 (3), 230–237.

Zhang, Z., Greene, B., Thuman-Commike, P.A., Jakana, J., Prevelige Jr., P.E., King, J., Chiu, W., 2000. Visualization of the maturation transition in bacteriophage P22 by electron cryomicroscopy. J Mol Biol 297 (3), 615–626.